The Journal of Experimental Biology 208, 3957-3969
Published by The Company of Biologists 2005
doi:10.1242/jeb.01858

Electrical properties and fusion dynamics of *in vitro* membrane vesicles derived from separate parts of the contractile vacuole complex of *Paramecium multimicronucleatum*

Kazuyuki Sugino*, Takashi Tominaga†, Richard D. Allen and Yutaka Naitoh‡

Pacific Biomedical Research Center, Snyder Hall 306, University of Hawaii at Manoa, 2538 The Mall, Honolulu, HI 96822, USA

*On leave of absence from the Institute of Basic Medical Sciences, University of Tsukuba, Tenno-Dai 1-1-1, Tsukuba 305-8575, Japan
†Present address: Laboratory for Brain-Operative Devices, Brain Science Institute (BSI), The Institute of Physical and Chemical Research (Riken), 2-1 Hirosawa Wako, Saitama 351-01, Japan
‡Author for correspondence (e-mail: naitoh@pbrc.hawaii.edu)

Accepted 24 August 2005

Summary

The contractile vacuole complex of *Paramecium multimicronucleatum* transforms into membrane-bound vesicles on excision from the cell. The *I–V* relationship was linear in a voltage range of –80 to +80 mV in all vesicles, despite being derived from different parts of the contractile vacuole complex. No voltage-gated unit currents were observed in membrane patches from the vesicles. Vesicles derived from the radial arm showed a membrane potential of >10 mV, positive with reference to the cytosol, while those derived from the contractile vacuole showed a residual (<5 mV) membrane potential. The electrogenic V-ATPases in the decorated spongiome are responsible for the positive potential, and Cl^- leakage channels are responsible for the residual potential. The specific resistance of the vesicle membrane (~6 kΩ cm^2) increased, while the membrane potential shifted in a negative direction when the vesicle rounded. An increase in the membrane tension (to ~5×10^{-3} N m^{-1}) is assumed to reduce the Cl^- leakage conductance. It is concluded that neither voltage- nor mechano-sensitive ion channels are involved in the control of the fluid segregation and membrane dynamics that govern fluid discharge cycles in the contractile vacuole complex.

The membrane vesicles shrank when the external osmolarity was increased, and swelled when the osmolarity was decreased, implying that the contractile vacuole complex membrane is water permeable. The water permeability of the membrane was 4–20×10^{-7} μm s^{-1} Pa^{-1}. The vesicles containing radial arm membrane swelled after initially shrinking when exposed to higher external osmolarity, implying that the V-ATPases energize osmolyte transport mechanisms that remain functional in the vesicle membrane. The vesicles showed an abrupt (<30 ms), slight, slackening after rounding to the maximum extent. Similar slackening was also observed in the contractile vacuoles *in situ* before the opening of the contractile vacuole pore. A slight membrane slackening seems to be an indispensable requirement for the contractile vacuole membrane to fuse with the plasma membrane at the pore. The contractile vacuole complex-derived membrane vesicle is a useful tool for understanding not only the biological significance of the contractile vacuole complex but also the molecular mechanisms of V-ATPase activity.

Key words: contractile vacuole complex, membrane vesicle, membrane potential, membrane resistance, membrane dynamics, membrane tension, patch clamp, water permeability, V-ATPase, *Paramecium multimicronucleatum*.

Introduction

The contractile vacuole complex (CVC) of *Paramecium multimicronucleatum* consists of a central contractile vacuole (CV) surrounded by 5–10 radial arms. A radial arm consists of (i) an ampulla, which connects with the CV, (ii) the collecting canal, which is continuous with the ampulla, (iii) the smooth spongiome meshwork that branches from the collecting canal and (iv) the decorated spongiome tubules, which are continuous with the smooth spongiome and end blindly in the cytosol (Hausmann and Allen, 1977; Allen and Naitoh, 2002). The CV is held in place against a permanent indentation of the cell surface membrane, the CV pore, by microtubular ribbons. The radial arms are also held in place next to the CV and near the cell surface by the same microtubular ribbons (McKanna, 1973; Hausmann and Allen, 1977).

Excess cytosolic water is translocated into the lumen of the CVC in association with transport of cytosolic osmolytes, most likely K^+ and Cl^- (Stock et al., 2002a,b). The transport is assumed to be energized by the electrogenic V-ATPase activity in the decorated spongiome membrane (Allen and Fok, 1988; Ishida et al., 1993, 1996; Fok et al., 1995; Merzendorfer et al.,

1997; Tominaga et al., 1998a,b; Wieczorek et al., 1999; Grønlien et al., 2002; Iwamoto et al., 2004). The fluid flows into the CV through collecting canals, causing the CV to swell (the fluid-filling phase). After a certain length of time the CV begins to round and the radial arms detach from the CV (the rounding phase). The ampullae begin to swell immediately after detachment of the radial arms, since the cytosolic water is continuously translocated into the lumen of the radial arm. At the end of the rounding phase the CV membrane fuses with the plasma membrane at the CV pore and the pore opens. The CV fluid is pushed out of the CV through the open pore by cytosolic pressure (Naitoh et al., 1997a,b), and the CV collapses and becomes microscopically invisible (the fluid-discharging phase). Immediately after fluid discharge the pore closes as the CV membrane is separated from the plasma membrane at the pore. The radial arms then reattach to the CV, so that the ampullae collapse while the CV swells. The CV continues to swell as fluid flows into it from the collecting canals (next fluid-filling phase).

Tominaga et al. (1999) found that the vesicles derived from the fragmented membrane of the CVC in mechanically ruptured cells continue to show rounding and slackening cycles but the vesicle cycles occur at different intervals, i.e. they are out of phase one with the other. This finding implies that the CVC membrane itself possesses a mechanism(s) by which its tension is periodically altered. Using a microcantilever placed on the surface of a CVC membrane vesicle, Tani et al. (2002) directly measured the tension of the vesicle membrane and found that the tension increased to ~5 mN m^{-1} as the vesicle rounded, and then returned to ~0.1 mN m^{-1} as the vesicle slackened.

Based on these findings we proposed a hypothesis that periodic changes in the CVC membrane tension govern the timing of the fluid discharge cycles of the CVC. That is, an increase in the tension leads to severing of the radial arms from the CV and to rounding of the CV, followed by opening of the pore that leads to CV fluid discharge. Conversely, a decrease in the tension causes closure of the pore and reattachment of the radial arms to the CV at the start of the fluid-filling phase (Allen and Naitoh, 2002; Tani et al., 2002).

Tani et al. (2000) demonstrated that fusion of two CVC membrane-derived vesicles with different periods of rounding–slackening occurred when both vesicles were in their slackening phases and the period of rounding–slackening cycles after fusion was closest to that of the fusing vesicle that had the shorter period. They also demonstrated that the CVC membrane-derived vesicle exhibited an extra rounding in response to suction of a small portion of the membrane into a micropipette when the vesicle was in the slackening phase. These findings support the idea that the mechanism(s) in the CVC membrane that controls the membrane tension is mechano-sensitive.

The primary objectives of the present study were to examine the presence of specific ion channels in the CVC membrane, i.e. (i) mechano-sensitive ion channels that are postulated to be involved in the control of tension development in the membrane and (ii) voltage-sensitive ion channels that are postulated to be involved in the control of the fluid segregation mechanisms energized by the electrogenic V-ATPase. Conventional patch-clamp techniques were employed for the present study (Ogden, 1994; Rudy and Iverson, 1992). Besides data on channels in the CVC membrane, we found some interesting CVC-derived membrane dynamics, which are also described in this paper.

Materials and methods

Cells

Paramecium multimicronucleatum (syngen 2; Allen and Fok, 1988) cells were grown in an axenic culture medium (Fok and Allen, 1979), of osmolarity approximately 84 mOsmol l^{-1} (Ishida et al., 1993) at 25°C. The cells were harvested at mid-logarithmic growth phase and washed with artificial cytosol (see the next section) containing polystyrene beads (2 μm in diameter) for 10 min before use in experiments. This procedure made it possible to tell the CVC-derived membrane vesicles from polystyrene bead-containing food vacuoles.

Experimental solutions

Artificial cytosol

The cytosolic osmolarity was found to be ~160 mOsmol l^{-1} (Stock et al., 2001) and the cytosolic KCl concentration was ~40 mmol l^{-1} (Stock et al., 2002b) in *Paramecium* cells growing in a standardized medium of ~ 80 mOsmol l^{-1}. Therefore, a mixture (mmol l^{-1} final concentration) of 40 KCl, 10 $MgCl_2$, 1 EGTA, 50 sorbitol and 10 Hepes (pH 7.0) was used as an artificial cytosol for the reference electrode.

Artificial CV fluid

The cytosolic KCl concentration was ~80 mmol l^{-1} (Stock et al., 2002b). The osmolarity of the CV fluid was assumed to be equal to the cytosolic osmolarity (Tominaga et al., 1998b). Therefore a mixture of 80 mmol l^{-1} KCl and 10 mmol l^{-1} Hepes (pH 7.0; Stock et al., 2002a) was used for the patch electrode as an artificial CV fluid.

Osmolarity-changing solution

A solution of 3 mol l^{-1} KCl, 2 mol l^{-1} sorbitol or 0.5 mol l^{-1} sorbitol was used to increase and distilled water to decrease the external osmolarity around the vesicle.

Assembly of the experimental apparatus

All experiments were performed on the stage of an inverted microscope (Leitz DMIRB, Leica Mikroskopie und Systeme GmbH, Wetzlar, Germany) placed on a vibration-free table (LW 3030B-OPT, Newport Corp., Irvine, CA, USA) at a regulated room temperature of approximately 25°C. Five micromanipulators (one PCF 5000, Burleigh Instruments, Inc., Fishers Victor NY, USA and four MHW-3, Narishige Group, East Meadow, NY, USA) were used for cell incision and manipulation of the extruded CVC-derived membrane vesicles. A VCR (Panasonic ACC 6300, Matsushita Electric

Inc., Osaka, Japan) and a CCD camera (CCD-72, DAGE MIT, Michigan City, IN, USA) were used for continuous recording of the images of incised cells and their CVC membrane vesicles during experimentation, so that the origin of the membrane vesicle being studied could be distinguished. A patch-clamp amplifier (EPC-8, Hekaelektronik, Lambrecht, Germany) and computer interface (ITC-16, Instrutech Corp., Great Neck, NY, USA) were employed. A computer (Macintosh Power Mac G4, Apple Computer Inc., Cupertino, CA, USA) was used to control experiments and for acquisition and subsequent analysis of the data.

Experimental procedures

Extrusion of the CVC-derived membrane vesicles from the cell

Paramecium cells were introduced into a mineral oil droplet on a coverslip together with a minute amount of axenic culture medium. Excess culture medium surrounding the cell was removed using a suction micropipette (approximately 3 μm i.d.) until the cells were compressed and flattened by the mineral oil–artificial cytosol boundary tension. The plasma membrane adjacent to the CV was incised using a microneedle. The CVC was extruded together with the cytosol through the incision by cytosolic pressure (Naitoh et al., 1997a,b). Sometimes the microneedle was needed to push the CVC out of the cell through the incision. The extruded CVC was always transformed into several membrane-bound vesicles (Tominaga et al., 1998b).

Patch-clamp experiments

The tip of a reference electrode (approximately 3 μm i.d.) filled with artificial cytosol was placed in the extruded cytoplasm. The tip of a patch-clamp pipette filled with artificial CVC fluid was first placed in the mineral oil surrounding the extruded cytoplasm containing the CVC membrane vesicles. A slight positive hydrostatic pressure was applied to the inside of the patch pipette, so that the artificial CV fluid was gently pushed out of the pipette when its tip was moved into the extruded cytosol from the surrounding mineral oil. The tip was then gently moved toward a membrane vesicle. When the tip touched the surface of the membrane vesicle, the overall electrode resistance slightly increased. A slight negative pressure was then applied to the inside of the pipette, so that the membrane of the vesicle became firmly attached to the opening of the pipette. In favorable preparations the overall electric resistance increased to the giga-seal level in several seconds. Voltage-clamp experiments in the on-vesicle patch-clamp mode were then performed. To perform experiments in the whole-vesicle patch-clamp mode, a minute negative pressure was further applied to the pipette until the overall electric resistance of the patch electrode suddenly decreased to a value comparable to the input resistance of the vesicle.

Changing the osmolarity around the CVC membrane vesicles

The tip (~5 μm i.d.) of a micropipette filled with the osmolarity-changing solution was placed close to the CVC membrane vesicle and the solution was ejected over several seconds by gently raising the hydrostatic pressure inside the pipette.

Results

The I–V *relationships of the membrane vesicles obtained from different portions of the CVC*

To examine whether the electrical characteristics of the membrane vesicles are different among vesicles derived from different portions of the CVC, shifts in membrane potential caused by injection of electric currents of varied intensity (the *I–V* relationship) were determined in different vesicles under the whole-vesicle patch-clamp mode. The CVC vesicles frequently fused with each other in different combinations.

The *I–V* relationship was linear in a voltage range between –80 and +80 mV in all vesicles examined (>20). Most of the vesicles showed the membrane potential (the potential at zero current) to be positive with reference to the excised cytosol (5–40 mV). Vesicles formed from only the CV membrane showed little membrane potential (less than 5 mV).

Representative results obtained from two different cells are shown in Fig. 1. As shown in Fig. 1Ai*a*, three small, radial arm-derived vesicles (identified by blue dots) and a larger CV-derived vesicle (red dot) were seen immediately after incision of the cell. These 'blue' vesicles were then topographically separated from the 'red' vesicle by placing a microneedle between them to prevent their fusion, as shown in Fig. 1Ai*b*.

The *I–V* relationship for the CV-derived vesicle ('red' vesicle in Fig. 1Ai*c*) is shown as a red line labeled *c* in Fig. 1Aii. The slope of the line corresponds to the vesicle's input resistance R_m of ~113 MΩ. The intersection of the red line with the *x*-axis (voltage) at current 0 corresponds to the vesicle's membrane potential V_m of ~1.2 mV. The three radial arm-derived vesicles (identified by blue dots) in Fig. 1Ai*a*,*b* fused into a large vesicle ('blue' vesicle in Fig. 1Ai*d*). The *I–V* relationship for this vesicle is shown as a blue line labeled *d* in Fig. 1Aiii. The input resistance and the membrane potential estimated from the intersection of the line are ~104 MΩ and ~11 mV, respectively.

As shown in Fig. 1Bi*e*, a large 'blue' vesicle formed by fusion of a CV with some radial arm vesicles lies near to two smaller 'blue' vesicles that formed from the membrane along two radial arms, respectively, immediately after cell incision. These three 'blue' vesicles later fused into a large vesicle (a 'blue' vesicle in Fig. 1Bi*f*). A 'red' vesicle in Fig. 1Bi*e* is the other CV of the cell and was in the rounding phase, becoming detached from the radial arms at the moment of cell incision. The CV-derived vesicle is shown in Fig. 1Bi*f* as a 'red' vesicle.

The *I–V* relationship for the 'blue' vesicle in Fig. 1Bi*f* is shown as a blue line labeled *f* in Fig. 1Bii. The input resistance and the membrane potential estimated from the line were ~70 MΩ and ~20 mV, respectively. This 'blue' vesicle later fused with the CV-derived vesicle (Fig. 1Bi*g*) into a larger vesicle (labeled half blue, half red in Fig. 1Bi*h*). The *I–V* relationship for the fused vesicle is shown as a half-blue, half-

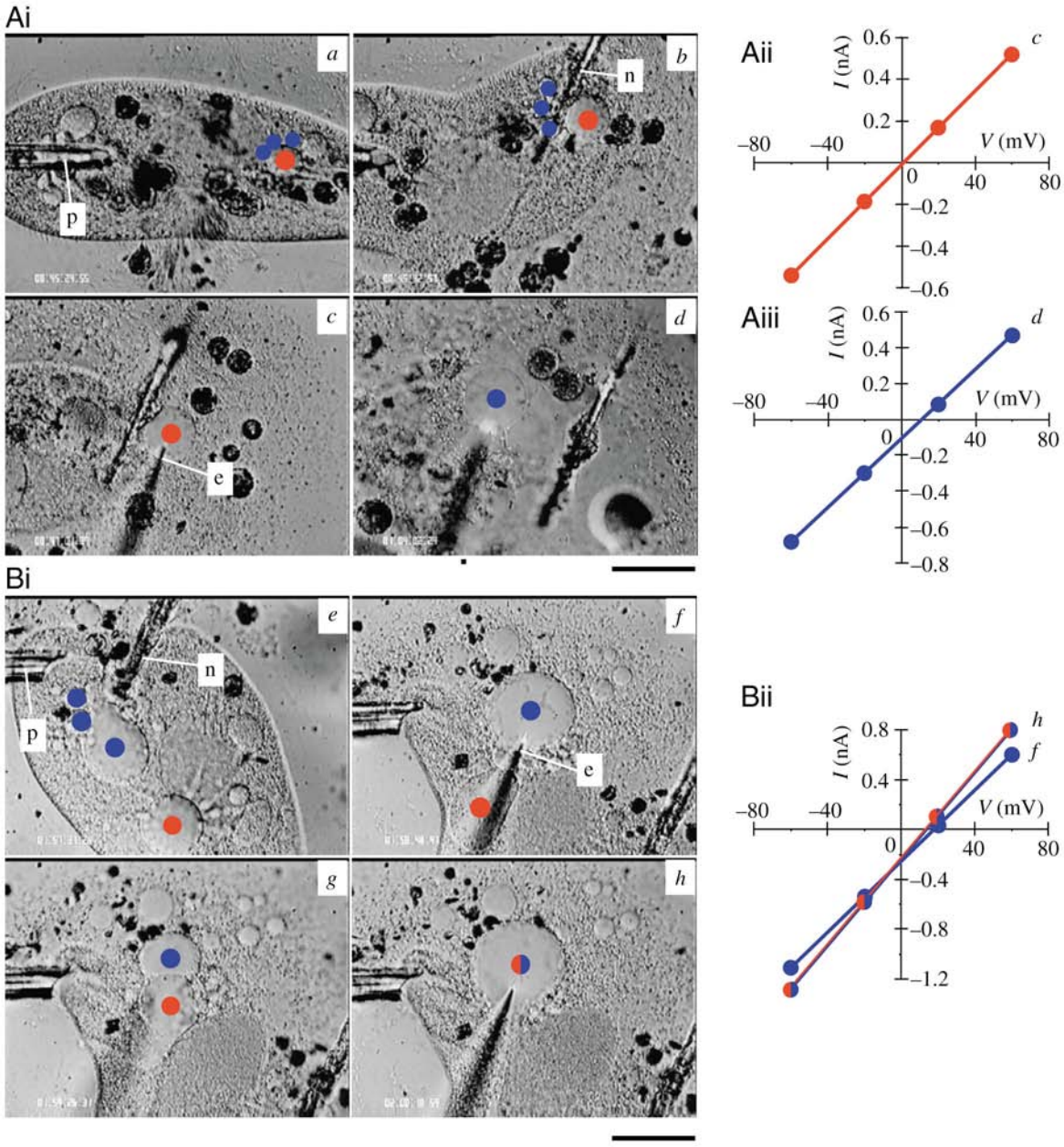

Fig. 1. Two series of pictures of the contractile vacuole complex-derived membrane vesicles obtained from two different *P. multimicronucleatum* cells (Ai, Bi). (Aii, Aiii, Bii) The *I–V* relationships for different membrane vesicles in Ai and Bi. Ai, Bi reveal the portion of the contractile vacuole complex from which each vesicle is derived. n, a microneedle used for incision of the cell or for preventing fusion of the membrane vesicles; p, suction pipette for removing solution around the cell; e, patch-clamp electrode. Scale bars, 50 μm. See the text for details.

red line labelled *h* in Fig. 1Bii. The input resistance and the membrane potential for the vesicle estimated from the line were ~58 MΩ and ~14 mV, respectively.

The electrical characteristics of a membrane patch from the membrane vesicle examined in the on-vesicle patch-clamp mode

Membrane currents generated in a membrane patch on a CVC-derived membrane vesicle in response to voltage steps varied in the range –80 to +80 mV were examined in the on-vesicle patch-clamp mode. As shown in Fig. 2, no voltage-gated current was observed in the membrane patch. In all vesicles tested no membrane patches were found that showed voltage-gated unit currents.

Changes in the input resistance and the membrane potential of membrane vesicles that show spontaneous rounding-slackening

I–V relationships of CVC membrane vesicles that show spontaneous rounding and slackening were determined and the images of the vesicles simultaneously tape-recorded. Two representative results obtained with two vesicles having

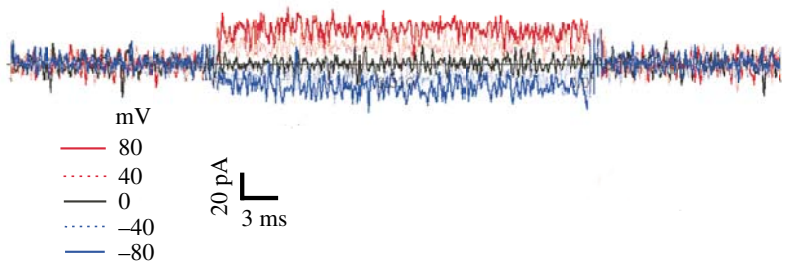

Fig. 2. Current responses in a membrane patch of the contractile vacuole complex-derived membrane vesicle obtained from a *P. multimicronucleatum* cell under on-vesicle patch-clamp mode. The five traces show the membrane currents generated in response to a clamped voltage in the range –80 to +80 mV.

different membrane potentials are shown in Fig. 3 (Fig. 3Ai,Aii,Aiii; ~10 mV; Bi,Bii,Biii; <~5 mV). The input resistance (Fig. 3Aii,Bii) and the membrane potential (Fig. 3Aiii,Biii) of the vesicles were estimated from the *I–V* relationships. The input resistance fluctuated in a range of less than 30% of its highest value and the membrane potential fluctuated in a range of less than 5 mV in all the vesicles examined.

In Fig. 3Ai, *e* and *f* correspond to the vesicle's maximum rounding and the start of slackening, respectively. Although the relationship between changes in R_m and V_m accompanied by rounding–slackening of the vesicle is rather ambiguous, R_m tended to increase as the vesicle rounded (Fig. 3Ai*a–e*), while V_m decreased when the vesicle showed maximum rounding (Fig. 3Aiii*d,e*). Inversely, R_m decreased (Fig. 3Aii*e–g*), while V_m increased (Fig. 3Aiii*e–g*) as the vesicle slackened.

Fig. 3Bi*a* corresponds to the slackening state of this vesicle. The vesicle started to round (Fig. 3Bi*a–g*) and finally ruptured

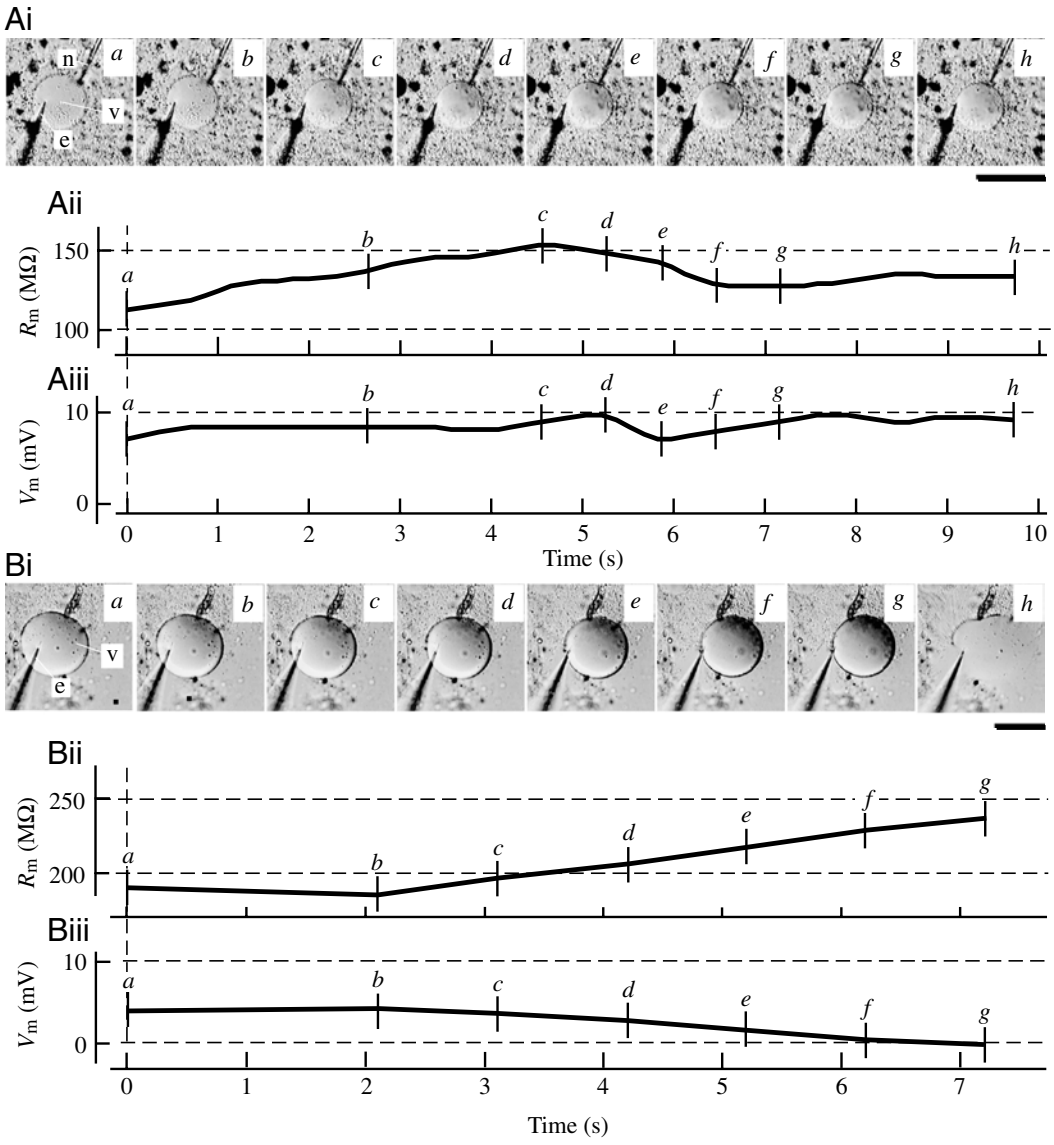

Fig. 3. Changes in the input resistance and the membrane potential of a membrane vesicle derived from the contractile vacuole complex of a *P. multimicronucleatum* cell accompanied by images of the vesicle's rounding-slackening. (Ai, Bi) Frames of two different vesicles showing rounding and slackening. Rounding of the vesicle is recognizable by the enhanced shadow effect (maximum rounding in Ai is in *e* and in Bi is in *g* before bursting in *h*). (Aii, Bii) Time courses of change in the input resistance, R_m, for the vesicles. (Aiii, Biii) Time courses of change in the membrane potential, V_m, for the vesicles. (*a–h*) in Ai and Bi correspond to the sequence when each picture was taken, which is also indicated by short vertical bars marked by the letters on the traces for R_m (Aii, Bii) and V_m (Aiii, Biii). e, patch-clamp electrode; n, microneedle; v, membrane vesicle. Scale bars, 50 μm.

(Fig. 3Bi*h*). R_m continued to increase (Fig. 3Bii*b–g*), while V_m continued to decrease (Fig. 3Biii*b–g*) as the degree of rounding increased with time until the vesicle ruptured. It should be noted that V_m became slightly negative immediately before the vesicle's rupture.

Change in vesicle volume after changing the surrounding osmolarity

To examine whether the CVC membrane is permeable to water, the osmolarity of the excised cytosol surrounding the membrane vesicles was changed by applying a more concentrated solution of solutes (3 mol l^{-1} KCl or 1 mol l^{-1} or 0.5 mol l^{-1} sorbitol) or distilled water to the cytosol through a micropipette placed close to the vesicles, at the same time that images of the vesicles were continuously video-recorded for subsequent estimation of vesicle volume.

Decreasing the osmolarity

When the surrounding cytosol was diluted by distilled water, all vesicles swelled to an extent that depended on their initial size and the degree of cytosol dilution. When the cytosol was extensively diluted, vesicles ruptured after they had swelled to their maximum size. A representative result is shown in Fig. 4, where Fig. 4Ai shows a consecutive series of five frames of one vesicle and Fig. 4Aii the time course of swelling of the vesicle after cytosol dilution. Vesicle volume increased to a stationary level of ~2.5 times larger than the initial level ~130 s after the start of dilution.

Increasing the osmolarity

When a more concentrated solution of solutes was added to the surrounding cytosol, all the vesicles decreased in size, depending on their initial sizes and the final osmolarity of the solution. When the final osmolarity was very high, the vesicles decreased in size until they became almost invisible. A representative result is shown in Fig. 4, where Fig. 4Bi shows a series of five consecutive frames of the vesicle and Fig. 4Bii shows the time course of shrinkage of the vesicle after

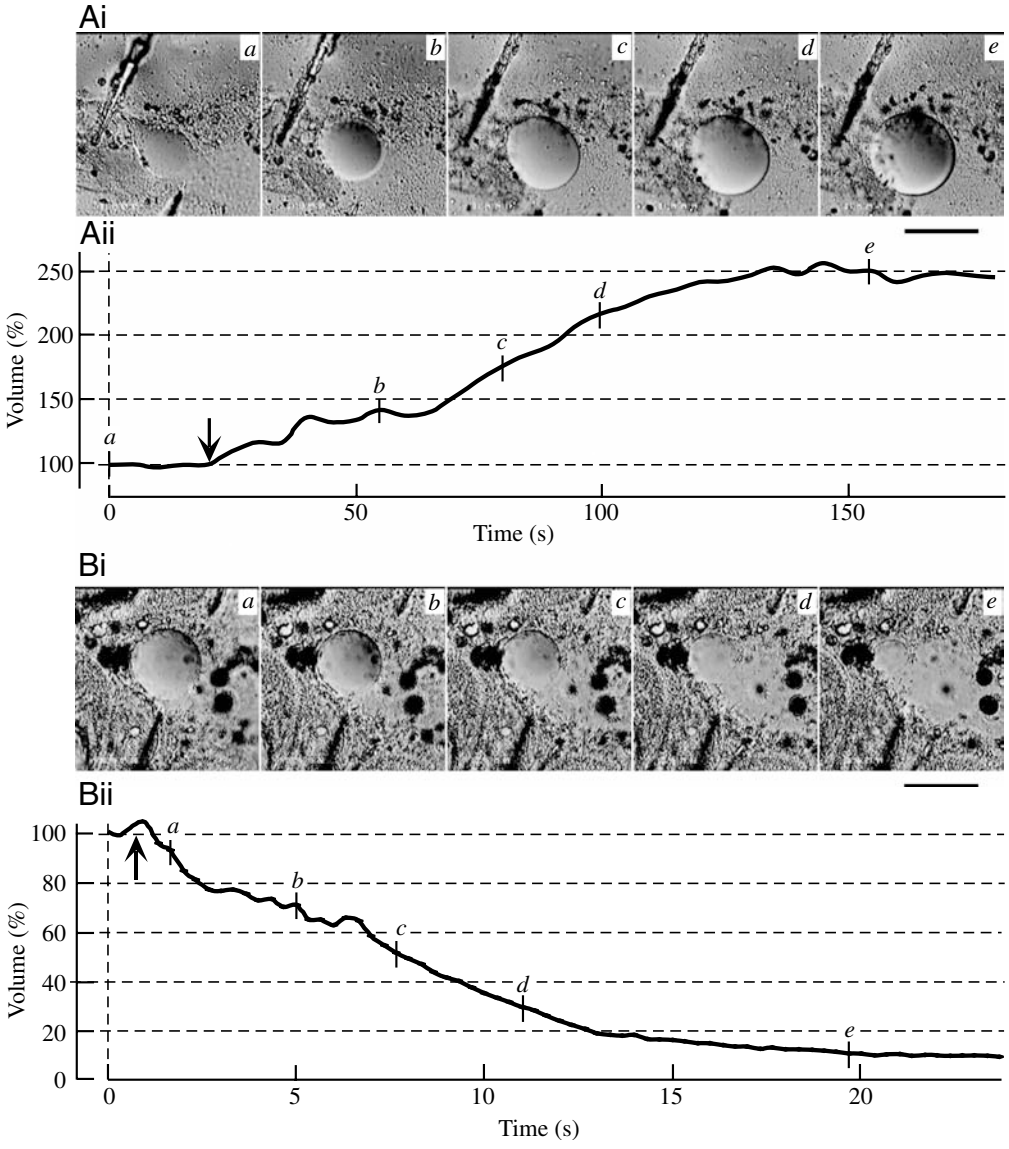

Fig. 4. Changes in the volume of membrane vesicles derived from the contractile vacuole complex of *P. multimicronucleatum* cells produced by a change in the external osmolarity. (Ai) A series of pictures of a vesicle that showed swelling after application of distilled water to the surrounding solution. (Aii) Time course of osmotic swelling of the vesicle shown in Ai. (Bi) A series of pictures of a vesicle that showed shrinkage after application of 3 mol l^{-1} KCl to the external solution. (Bii) Time course of osmotic shrinkage of the vesicle shown in Bi. Arrows in Aii and Bii show the time when the external osmolarity was changed. Letters *a–e* on each graph show the times when the pictures in the corresponding frames in Ai and Bi were taken. Vesicle volume is presented as the percentage of that before changing the external osmolarity. Scale bars, 50 μm.

increasing the external osmolarity. The volume of the vesicle decreased to a stationary level of ~1/10 of the initial level ~20 s after the increase in the osmolarity.

Reswelling of the membrane vesicles held in an increased external osmolarity

The membrane vesicle was found to be able to swell again after it had decreased in volume in an increased osmolarity. Some vesicles even ruptured after they had reached their respective maximum sizes. A representative result is shown in Fig. 5, where Fig. 5A*a–f* shows a consecutive series of frames of a vesicle in which the volume increases; Fig. 5B shows the time course of increase in volume of the vesicle after it had first reached its minimum level in an increased external osmolarity. Vesicle volume increased almost linearly with time to its maximum level in approximately 40 min, then gradually decreased to a stationary level of a little lower than the maximum level (Fig. 5*g–j*). Examination of the origin of the membrane from their video-recorded images revealed that the vesicles deriving membrane from only CV showed no reswelling when subjected to an increased osmolarity.

It was sometimes observed that the reswelling of the vesicle in solutions of increased osmolarity ceased concomitantly with cessation of beating of the cilia on the fragmented plasma membrane that frequently appeared in the extruded cytosol together with the vesicles. Our preliminary experiment showed that both ciliary beating and reswelling of the vesicle resumed after an addition of ATP to the excised cytosol.

Fusion of vesicles follows osmotic shrinkage

The CVC-derived membrane vesicles ended up more or less rounded when they were kept immersed in the excised cytosol for more than 1 h. They did not fuse with each other after they had rounded. When a more concentrated solution of solutes was added to the extruded cytosol, the rounded vesicles decreased in volume osmotically and some of them were then able to fuse with their neighboring vesicles. A representative series of consecutive pictures of the vesicles that showed fusion after increasing the surrounding osmolarity is shown in Fig. 6.

As shown in Fig. 6, frame 0 (the number in the upper right of the frame corresponds to the time in seconds when each picture was taken after initiating the osmolarity increase), four more-or-less rounded vesicles, labeled 1–4, sit close to each other, but are not fused. The vesicles decreased in size and flattened in response to increasing the external osmolarity (Fig. 6, frames 0.04–0.7), then vesicles 2 and 3 fused with each

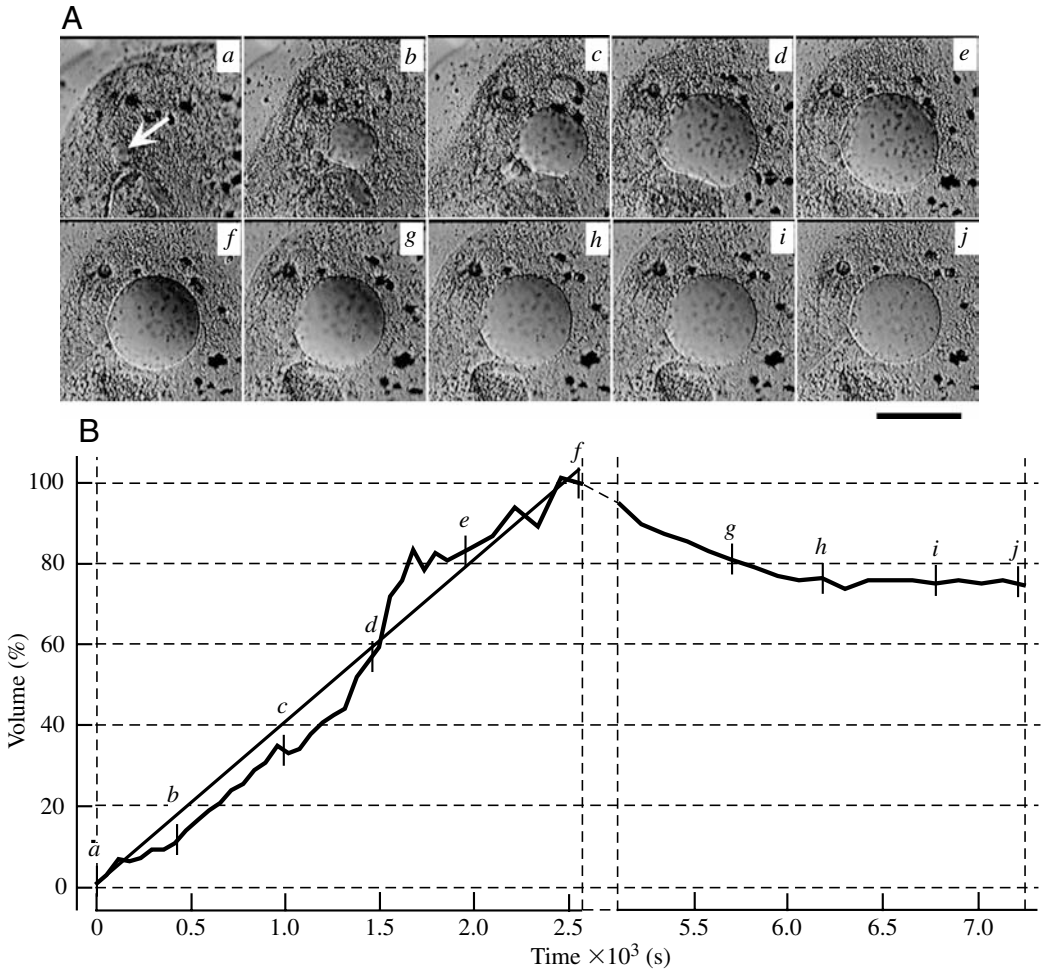

Fig. 5. Swelling of a vesicle derived from the contractile vacuole complex of a *P. multimicronucleatum* cell that took place after the vesicle had previously decreased to its minimum size in an increased external osmolarity of 1 mol l^{-1} sorbitol. (A) A series of pictures of the vesicle showing swelling. The white arrow in *a* points to the shrunken vesicle. (B) Time course of swelling of the vesicle. Vesicle volume is presented as the percentage of its maximum volume in the increased osmolarity. Letters *a–j* in B show the times when the pictures in the corresponding frames in A were taken. The straight line is the linear approximation of the increase in vesicle volume. Scale bar, 50 μm.

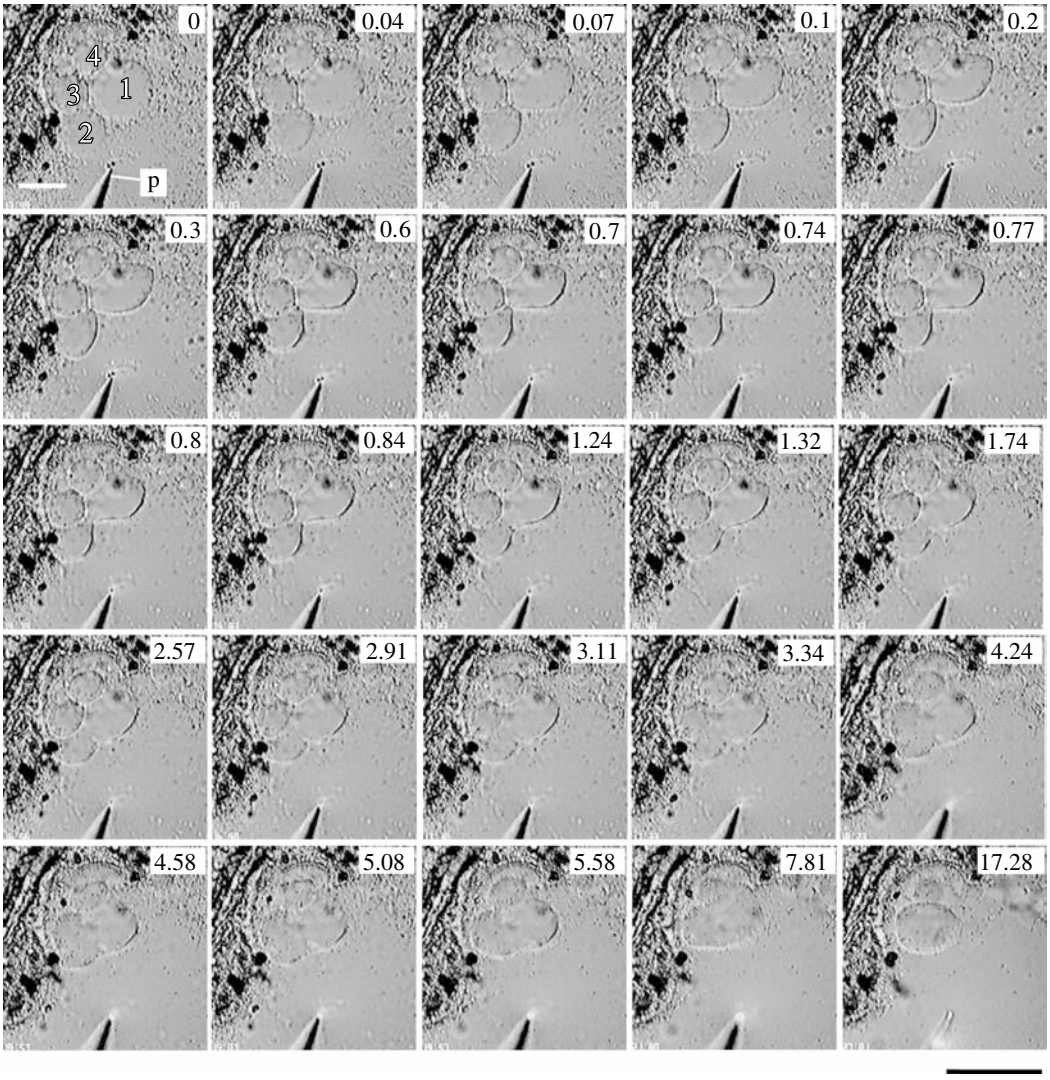

Fig. 6. A series of pictures of four (labelled 1–4 in frame 0) membrane vesicles derived from the contractile vacuole complex of a *P. multimicronucleatum* cell, showing shrinkage and subsequent fusion when exposed to an increased external osmolarity produced by adding 0.5 mol l^{-1} sorbitol solution. Numbers on frames correspond to the time (s) when the picture was taken after the start of the increase in external osmolarity. p, a micropipette for application of the sorbitol solution. Scale bar, 10 μm.

other (Fig. 6, frames 2.91–4.24). This fused vesicle then fused with vesicle 1 (Fig. 6, frames 4.24–7.81).

An abrupt slight slackening was seen immediately after the degree of rounding reached its maximum in both in vitro *CVC-derived vesicles and in the* in situ *CVs*

The CVC-derived membrane vesicles were found to show an abrupt slight slackening immediately after maximum rounding, which was then followed by a more gradual slackening. The abrupt slackening was detected as a slight increase in the area of the image of the rounded vesicle after removing the surrounding cytosol and thereby strongly compressing the vesicle under the mineral oil–cytosol boundary tension. A representative result is shown in Fig. 7, where Fig. 7Ai shows pictures of the vesicle and Fig. 7Aii the time course of change in the area of the vesicle's image. Fig. 7A*i*b,*c* correspond to the vesicle's maximum rounding and abrupt slackening, respectively. These pictures were obtained from two consecutive frames in a tape-recorded series of images, so that the abrupt slackening took place within the time required to produce a single frame (<30 ms). The slackening was visible to the naked eye as a faint flicker during a replay of the tape-recorded images, although the difference in the still pictures between *b* and *c* is inconspicuous. The abrupt increase in the area is clearly shown in the inset graph of Fig. 7Aii, where the expanded time course is shown as a red line. Red circles on the red line in the inset labeled *b*, *c* and *d*, respectively, correspond to the time when each corresponding picture was taken. It is clear from the inset that the abrupt increase took place between *b* and *c*, as indicated by an arrowhead labeled S.

To examine whether an abrupt slackening takes place also in the *in situ* CV, a *Paramecium* cell was compressed under a coverslip (~5 μm thick space) so that the CV inside the cell was flattened. The compressed CV's image was tape-recorded during its fluid discharge cycles. A representative result is shown in Fig. 7B*i*a–*j* and Fig. 7Bii (the time course of change in the area of the image of the CV). Similarly to the CVC-derived membrane vesicles, the *in situ* CV showed an abrupt slackening immediately after maximum rounding. The abrupt

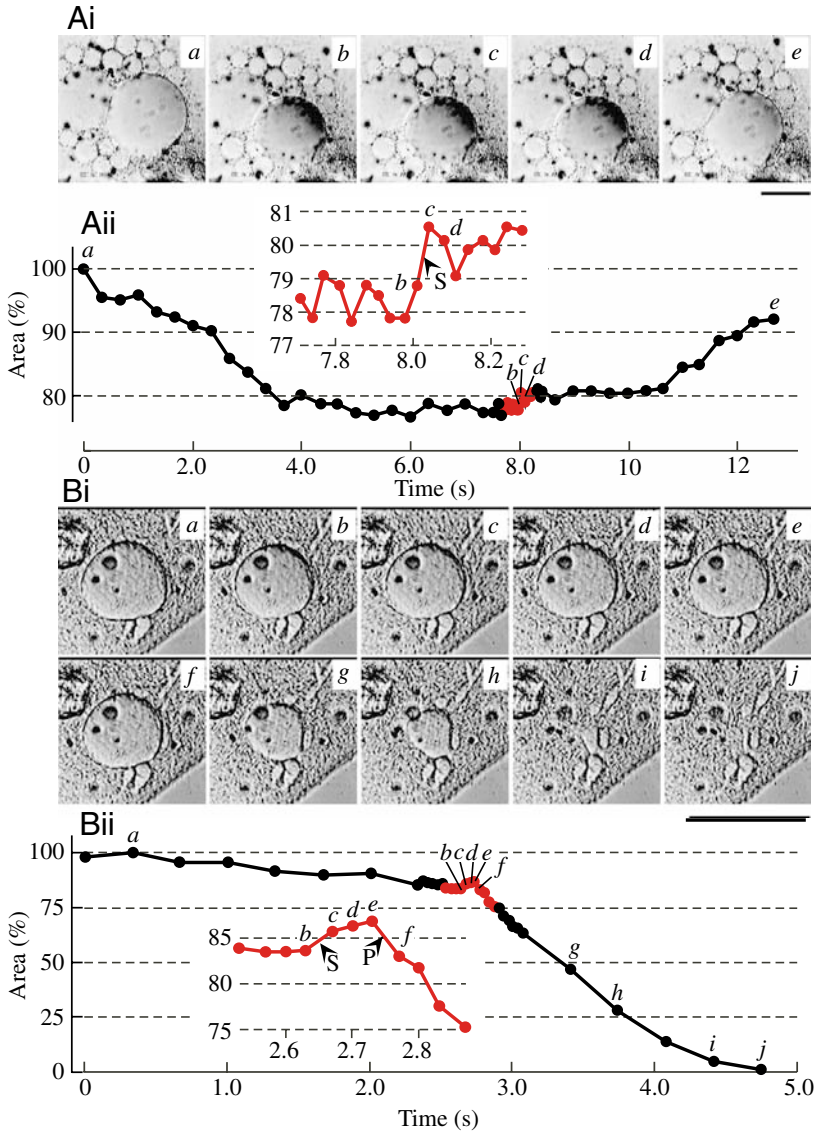

Fig. 7. An abrupt slackening in the membrane vesicle (Ai) derived from the contractile vacuole complex and the contractile vacuole (Bi) from *P. multimicronucleatum* cells. (Aii, Bii) Time course of change in the area of the image of the vesicle and the CV, respectively. Areas are presented as the percentage of the largest area achieved during the maximum degree of slackening prior to CV pore opening during the recording. Insets in Aii and Bii are expanded portions of the time courses presented in red. See the text for the details. Scale bars, 50 μm.

slackening was visible to the naked eye as a faint flicker during the replay of the tape-recorded images of the CV. The abrupt increase in the membrane area is depicted in the expanded time course shown as a red line in the inset of Fig. 7Bii. The increase commenced between the times that Fig. 7B*i*b and *c* were taken, respectively (red circles labeled *b* and *c*), and indicated by an arrowhead labeled S.

The abrupt increase was followed by a further increase in the area (red circles labeled *d* and *e* that correspond to Fig. 7B*i*d,*e*, respectively. The area then abruptly decreased to almost 0 (from *e* to *j* in both the pictures and the time course). This decrease in the area corresponds to the phase of discharge of the CV fluid through the CV pore. The pore opening, therefore, took place between *e* and *f*, as indicated by an arrowhead labeled P.

Discussion

Electrophysiological characteristics of the CVC-derived membrane vesicles

The radial arm-derived membrane is responsible for the membrane potential of the vesicle

We found that a membrane vesicle identified as derived from only the CV showed a residual membrane potential of <5 mV, positive with reference to the external excised cytosol (Fig. 1Aii). By contrast, the radial arm-derived vesicle showed a membrane potential of >10 mV (Fig. 1Aiii). Tominaga et al. (1998a,b) found that the V-ATPase that exclusively resides in the decorated spongiome along the radial arms (Allen at al., 1990; Fok et al., 1995) was electrogenic (see also Grønlien et al., 2002). The radial arm-derived vesicle is assumed to be composed of both the smooth spongiome and the decorated spongiome, so it will contain V-ATPases in its membrane that are the cause of the considerable membrane potential.

In fact, most of the CVC-derived membrane vesicles will contain membranes from both the smooth spongiome and the decorated spongiome, since both membranes are found along most of length of the radial arms and both will be incorporated in each vesicle derived from the radial arms that forms in the excised cytoplasm (Tani et al., 2000, 2001). We found that the membrane potential in these vesicles varied within a range 1–30 mV. The amplitude of the membrane potential is assumed to be proportional to the number of the V-ATPases relative to the overall vesicle membrane area (Grønlien et al., 2002). In fact, a membrane potential of ~20 mV for a vesicle derived from both the CV and radial arm membrane (a 'blue' vesicle in Fig. 1B*i*f) decreased to ~14 mV after the vesicle fused with another vesicle that was derived only from the CV, which means it did not contain V-ATPases ('red' vesicle in Fig. 1B*i*e–g), to form a larger vesicle ('half blue-half red' vesicle in Fig. 1B*i*h). The membrane potential of the vesicle corresponds to the point of intersection of the *I–V* plot for the vesicle (a blue line for the 'blue' vesicle and a half blue-half red line for the 'half blue-half red' vesicle in Fig. 1Bii) with the voltage axis. The *I–V* relationships also reveal that the input resistance (which corresponds to the slope of the *I–V* plot) of ~70 MΩ for the vesicle before fusion decreased to ~48 MΩ after fusion. This

decrease in the input resistance corresponds to an increase in the membrane area produced by the fusion. An electric current generated by the V-ATPases was shunted by an increased membrane area so that the membrane potential decreased.

Voltage-activated ion channels are not present in the CVC membrane

The *I–V* relationships for the vesicles in the whole-vesicle patch-clamp mode were always linear in a voltage range from –80 to +80 mV (Fig. 1Aii,Aiii,Bii). This implies that voltage-sensitive ion channels, gated by a membrane potential change within this range, are not present in the CVC membrane. Voltage-activated single-channel currents were not observed in the current traces for membrane patches in the on-vesicle patch-clamp mode (Fig. 2A). This strongly supports the idea that no voltage-activated ion channels are present in the CVC membrane. By employing a two-electrode current-clamp technique, Tominaga et al. (1998a) demonstrated that the *I–V* relationship for the CV in the rounding phase (a time when the CV is detached from the radial arm membrane) was straight in a voltage range from –60 to +60 mV and that it was also straight for the CV in the fluid-filling phase (a time when the CV is connected to the rest of the CVC) in a voltage range from –20 to +20 mV, and concluded that very few voltage-activated ion channels are present in any part of the CVC. The present study confirms this over a wider range of membrane voltage. By contrast, Yoshida et al. (1997) demonstrated a voltage- and K^+-dependent K^+ channel in an artificial lipid bilayer membrane into which a membrane fraction enriched in the CV membrane of *Dictyostelium discoideum* was incorporated. They suggest that the channels may play a role in the cytosolic water transport into the CV lumen of this cell.

Non-voltage-sensitive ion channels are present in the CVC membrane

The specific membrane resistances of the membrane vesicles were estimated (Table 1) with six different vesicles (two derived from the CV, two derived from the radial arm and two derived from a mixture of both the CV and the radial arm). The membrane areas of the vesicles were estimated based on the assumption that they were spherical when their *I–V* relationships were determined. The mean value for the specific resistance was $5.2\pm1.3\ 10^3\ \Omega\ cm^2$. This value is consistent with the value of $\sim5.7\ 10^3\ \Omega\ cm^2$ for the *in situ* CVC obtained by Tominaga et al. (1998a). This specific resistance value is within a range consistent with those for conventional cells, including *Paramecium* (Eckert and Naitoh, 1970; Fain, 1999), and indicates the presence of some non-voltage-sensitive ion channels in the membrane.

Residual positive membrane potential found in the vesicles derived from only the CV (Table 1) is assumed to be caused by the presence of these ion channels. By employing ion-selective microcapillary electrodes, Stock et al. (2002a,b) found that K^+ and Cl^- activities in the CV fluid were higher than those in the cytosol. It is, therefore, highly probable that Cl^- is responsible for generation of the residual membrane potential. The residual membrane potential was also observed in the *in situ* CV after detachment of the radial arms that occurs immediately before fluid discharge (Tominaga et al., 1998a,b). To identify the ion specificity of these channels, extensive examinations of the effects of various ion species and of differing concentrations on the vesicle membrane potential are needed.

Rounding and slackening of the vesicle modify the specific membrane resistance and the membrane potential of the vesicle

As is shown in Fig. 3, the input resistance increased, while the membrane potential shifted in a negative direction when the membrane vesicle rounded. Inversely, the input resistance decreased, while the membrane potential shifted towards a positive direction when the membrane vesicle slackened. Based on membrane capacitance measurements of the *in situ* CV, Tominaga et al. (1998b) found that the membrane area of the CV did not change during the CV's rounding. Therefore, an increase in the vesicle's input resistance corresponds to an increase in the specific membrane resistance of the vesicle and *vice versa*.

As was previously mentioned, Cl^- activity is higher in the CV fluid than the cytosol (Stock et al., 2002b). It is, therefore, probable that the shift of the membrane potential towards a negative direction is caused by a decrease in the Cl^- conductance of the membrane as the vesicle rounds. By using a microcantilever placed on the surface of an isolated CVC

Table 1. *Specific resistance of the contractile vacuole complex (CVC) membrane of* P. multimicronucleatum *estimated from the input resistance of the membrane vesicles derived from the CVC*

Vesicle no.	Fig.	Origin	V_m (mV)	D (μm)	A (μm^2)	R_m (MΩ)	R_{spc} (kΩ cm^2)
1	1Ai*c*	CV	1.2	30.9	3000	113	3.4
2	Not shown	CV	0.7	31.4	3090	242	7.5
3	1Ai*d*	RA	11.2	37.5	4420	104	4.6
4	1Bi*f*	RA	17.9	49.5	7710	70	5.4
5	1Bi*h*	CV+RA	14.1	54.0	9170	58	5.3
6	3A*e*	CV+RA	7.1	33.9	3620	142	5.1

CV, contractile vacuole; RA, radial arm; V_m, membrane potential; D, diameter of the vesicle; A, planar membrane area of the vesicle calculated from D; R_m, input resistance of the vesicle; R_{spc}, specific resistance of the vesicle membrane.

membrane vesicle, Tani et al. (2001) directly measured an increase in the membrane tension (a force generated by a vesicle) to ~5 mN m^{-1} (which corresponds to ~36 nN) during rounding from its lowest value of ~0.1 mN m^{-1} (which corresponds to ~1.8 nN) during vesicle membrane slackening. The membrane tension of ~5 mN m^{-1} that causes a decrease in the ion (presumably Cl^-) conductance of the vesicle membrane is much higher than the membrane tension that activates mechano-sensitive ion channels, i.e. ~1 mN m^{-1} (Gustin, 1992; Sokabe et al., 1991; Morris, 2001). It can, therefore, be concluded that there are no conventional mechano-sensitive ion channels in the CVC membrane. The mechanical distortion of the channel molecules by a high membrane tension would be expected to cause a decrease in the leakage conductance of the CVC membrane. According to Sheetz and Dai (1996), lytic tension for lipid bilayers approximates 2–10 mN m^{-1}, a value comparable to the highest tension generated by the CVC membrane vesicle. In fact, the *in vitro* CVC membrane vesicle is sometimes lysed after rounding (Fig. 3Bi*h*); it can be assumed that the membrane tension of the vesicle has exceeded the threshold for membrane lysis.

It was also noted that V_m sometimes became negative with reference to the cytosol as the vesicle rounded (Fig. 3Biii). This implies that some cations are involved in generating the membrane potential of the vesicle. K^+ is the most likely candidate for the negative potential (Stock et al., 2002b). K^+ leakage conductance is assumed to be less affected by the membrane tension, so that K^+ potential comes to predominate over Cl^- potential as the membrane tension increases.

Based on our electrophysiological examinations of the CVC membrane vesicles, we conclude that neither voltage- nor mechano-sensitive ion channels are involved in the mechanisms governing the transport of osmolytes energized by the V-ATPases and those controling the membrane dynamics associated with cyclic fluid discharge in the CVC.

The CVC membrane is water permeable

The *in vitro* CVC membrane vesicle swelled when the surrounding excised cytosol was diluted by distilled water (Fig. 4Ai,Aii), and shrank when the osmolarity of the cytosol was increased by adding 3 mol l^{-1} KCl (Fig. 4Bi,Bii) or 2 mol l^{-1} sorbitol (data not shown) to the cytosol. The degree of swelling was larger when the cytosol was more diluted. The vesicles ruptured after they had attained their respective maximum sizes when the extruded cytosol was extremely diluted. At the other extreme, the degree of shrinkage was larger when the osmolytes in the excised cytosol became more concentrated. The minimum size of the vesicles in a solution of increased osmolarity differed from one vesicle to the other. These results strongly support the idea that the CVC membrane is water permeable. The water permeability coefficient of the vesicle membrane estimated from the data shown in Fig. 4 approximated $4–20\times10^{-7}$ μm s^{-1} Pa^{-1}. This value suggests the presence of water channels (such as aquaporins) in the CVC membrane.

Tominaga et al. (1998a,b) proposed a hypothesis for fluid segregation in the CVC that V-ATPases in the decorated spongiome energize a hypothetical transport mechanism that conveys osmolytes from the cytosol into the CVC lumen. Water molecules are consequently osmotically transported from the cytosol into the CVC lumen through water channels that distribute throughout the CVC membrane. The osmolarity of the fluid in the CVC lumen is, therefore, virtually equal to that of the cytosol. Our present finding of water permeability of the membrane vesicle strongly supports this hypothesis.

Recently Nishihara et al. (2004) estimated the water permeability coefficient of the CV membrane in a freshwater amoeba *Amoeba proteus*, based on the rate of shrinkage of the isolated CV in a hyperosmotic solution of 3.8×10^{-7} μm s^{-1} Pa^{-1}. This value is strikingly similar to our value for the water permeability coefficient of the CVC of *Paramecium*. Based on this high value for the water permeability, they suggested the presence of water channels in the CV membrane of the amoeba. A recent study of the CVC in *Trypanosoma cruzi* demonstrated the presence of a functional aquaporin water channel in the CVC of this parasitic protozoan (Montalvetti et al., 2004).

Fluid segregation takes place in the in vitro *membrane vesicles*

We found that the volume of the CVC-derived membrane vesicles increased almost linearly with time after the vesicles had decreased to their minimum size when subjected to an increased osmolarity (Fig. 5B). This implies that the hypothetical V-ATPase-energized osmolyte transport mechanisms, which are present in the vesicle membrane, remain active after the vesicles have been subjected to an increased osmolarity, and may explain why some vesicles ruptured after attaining their respective maximum sizes (data not shown).

The rate of increase in vesicle volume was calculated from the slope of the linear approximation of the time course of change in vesicle volume (a solid straight line in Fig. 5B) and was found to be ~46.5 fl s^{-1}. This value is comparable to the rate of fluid segregation of a single CVC of an 84 mOsmol l^{-1}-adapted cell in its adaptation solution, i.e. ~45 fl s^{-1} (Stock et al., 2001).

Most of the *in vitro* membrane vesicles were found to swell in the extruded cytosol (data not shown). This swelling ceased concomitantly with cessation of ciliary beating, which requires ATP, on the fragmented plasma membranes in the cytosol. This implies that the swelling needs ATP. Our preliminary observation showed that application of ATP to the excised cytosol reactivated the vesicle volume increase concomitantly with reactivation of ciliary beating, implying that the V-ATPases incorporated into the membrane vesicle are responsible for the water transport from the cytosol into the vesicle lumen, as is also the case in the *in situ* CVC.

Some notable membrane dynamics in the in vitro CVC membrane vesicles

Osmotic shrinkage of the vesicles permits their fusion

Tani et al. (2000, 2001) found that the *in vitro* CVC

membrane vesicles ceased to show rounding–slackening cycles and became more-or-less rounded (the rigor state of the vesicle) when they were exposed to a lowered ATP concentration. They also found that two membrane vesicles showing rounding–slackening cycles with different cycle periods fused only when they both showed slackening at the same time. Fig. 6 clearly demonstrates that the *in vitro* CVC membrane vesicles in the rigor state (vesicles labeled 1, 2 and 3 in Fig. 6,0) fused with each other when they had slackened in response to an increased external osmolarity. These observations support the idea that the slackening of the membrane vesicle, i.e. a decrease in the membrane tension, is indispensable for membrane fusion, and ATP is not needed for fusion *per se*. The homotypic fusion process in the CVC membrane vesicles seems to be a purely physical phenomenon, as is the case for fusion between artificial lipid bilayer membrane vesicles.

Rounding of the membrane vesicle was always followed by a slight and abrupt slackening

Frame-by-frame analysis of the video-recorded images of a compressed membrane vesicle revealed that a slight increase in the area occupied by the vesicle's image took place immediately after its area had reached a minimum in a period of time corresponding to a single frame of the tape-recording (~30 ms; Fig. 7Aii). The increase was visible as a faint flicker to the naked eye in the replayed tape-recorded images of the vesicle. The minimum area corresponds to the vesicle at its maximum rounding, or the maximum membrane tension, and a subsequent slight increase in the image area corresponds to a slackening of the vesicle, or a slight decrease in the membrane tension.

By using a microcantilever placed on the surface of a membrane vesicle, Tani et al. (2001) directly measured cyclic changes in the membrane tension of the vesicle that accompanied its rounding-slackening cycles. Although they did not mention it, they clearly demonstrated this slight and abrupt decrease in the membrane tension from its maximum value of ~5 mN m^{-1} for the rounding phase to ~4.7 mN m^{-1} within ~0.4 s. This change was significant but so small that it was not discussed.

An extremely compressed membrane vesicle can be regarded as a right circular cylinder in shape. The relationship between the membrane tension and the area of the image of the vesicle compressed by a definite force can be formulated as:

$$T_s/T_r = \sqrt{(A_r/A_s)}\ ,$$

where T_r and T_s are the tension and A_r and A_s the area, immediately before and after the vesicle had changed from rounding to an abrupt slackening. The value for T_s/T_r calculated from the data presented in Tani et al. (2001) approximates 0.94. The value for $\sqrt{A_r/A_s}$ obtained from the values for A_s and A_r presented in Fig. 7Aii, approximates 0.98. This value is likely to be overestimated, since compression of the vesicle in the present experiment is insufficient to regard the vesicles to be ideal right circular cylinders. Consequently A_s would be underestimated. This abrupt increase in the area of the vesicle image is comparable to what would be expected of an abrupt decrease in the membrane tension.

An abrupt slackening after rounding was also observed in the in situ *CV*

As is shown in Fig. 7Bii, the area of the image of an extremely compressed *in situ* CV slightly increased in a period of time corresponding to a single frame of the video recording immediately after it had reached its minimum value, much like the *in vitro* CVC membrane vesicle. This implies that a slight and abrupt decrease in the membrane tension took place after the membrane tension had reached its maximum value (maximum rounding).

It is notable that the area increased more during the next two frames (for ~60 ms) after its abrupt increase (Fig. 7Bi*d*,*e*,Bii*d*,*e*), then decreased abruptly (Fig7Bi*f*, Bii*f*). This abrupt decrease corresponds to the start of fluid discharge from the CV, so that the CV area subsequently decreases to 0. The start of fluid discharge corresponds to fusion of the CV membrane with the plasma membrane at the cell's CV pore. We conclude that fusion takes place when the CV membrane tension has begun to decrease from its highest value that was reached at maximum rounding.

We had previously concluded (Tominaga et al., 1998b, 2000, 2001) that fusion of the CV membrane with the plasma membrane at the pore takes place when the CV membrane tension reached its maximum value. This hypothesis can now be corrected based on this new information to say that the CVC membrane fuses with other CVC membrane vesicles or with the pore membrane when the membrane tension has started to decrease. However, rounding accompanied by an increase in membrane tension of the CV to its highest value is indispensable for positioning the CV membrane topographically in the right place for its subsequent fusion with the pore membrane, a process aided by the cytoskeletal microtubular structures that bind to the CV and that surround the CV pore.

This work was supported by NSF grant MCB 01 36362. We thank Drs S. Ozawa and M. Tani for their valuable comments on the patch-clamp technique.

References

Allen, R. D. and Fok, A. K. (1988). Membrane dynamics of the contractile vacuole complex of *Paramecium*. *J. Protozool.* **35**, 63-71.

Allen, R. D. and Naitoh, Y. (2002). Osmoregulation and contractile vacuoles of protozoa. *Int. Rev. Cytol.* **215**, 352-394.

Allen, R. D., Ueno, M. S., Pollard, L. W. and Fok, A. K. (1990). Monoclonal antibody study of the decorated spongiome of contractile vacuole complex of *Paramecium*. *J. Cell Sci.* **96**, 469-475.

Eckert, R. and Naitoh, Y. (1970). Passive electrical properties of *Paramecium* and problems of ciliary coordination. *J. Gen. Physiol.* **55**, 467-483.

Fain, G. L. (1999). *Molecular and Cellular Physiology of Neurons*. Cambridge, MA, London: Harvard University Press.

Fok, A. K. and Allen, R. D. (1979). Axenic *Paramecium caudatum*. I. Mass culture and structure. *J. Protozool.* **26**, 463-470.

Fok, A. K., Aihara, M. S., Ishida, M., Nolta, K. V., Steck, T. L. and Allen, R. D. (1995). The pegs on the decorated tubules of the contractile vacuole complex of *Paramecium* are proton pumps. *J. Cell Sci.* **108**, 3163-3170.

Grønlien, H. K., Stock, C., Aihara, M. S., Allen, R. D. and Naitoh, Y. (2002). Relationship between the membrane potential of the contractile vacuole complex and its osmoregulatory activity in *Paramecium multimicronucleatum. J. Exp. Biol.* **205**, 3261-3270.

Gustin, M. C. (1992). Mechano-sensitive ion channels in yeast. Mechanism of activation and adaptation. *Adv. Compar. Environ. Physiol.* **10**, 19-38.

Hausmann, K. and Allen, R. D. (1977). Membranes and microtubules of the excretory apparatus of *Paramecium caudatum*. *Eur. J. Cell Biol.* **15**, 303-320.

Ishida, M., Aihara, M. S., Allen, R. D. and Fok, A. K. (1993). Osmoregulation in *Paramecium*: the locus of fluid segregation in the contractile vacuole complex. *J. Cell Sci.* **106**, 693-702.

Ishida, M., Fok, A. K., Aihara, M. S. and Allen, R. D. (1996). Hyperosmotic stress leads to reversible dissociation of the proton pump-bearing tubules from the contractile vacuole complex in *Paramecium*. *J. Cell Sci.* **109**, 229-237.

Iwamoto, M., Allen, R. D. and Naitoh, Y. (2004). Hypo-osmotic or Ca^{2+}-rich external conditions trigger extra contractile vacuole complex generation in *Paramecium multimicronucleatum*. *J. Exp. Biol.* **206**, 467-473.

McKanna, J. A. (1973). Fine structure of the contractile vacuole pore in *Paramecium*. *J. Protozool.* **20**, 631-638.

Merzendorfer, H., Graf, R., Huss, M., Harvey, W. R. and Wieczorek, H. (1997). Regulation of proton-translocating V-ATPases. *J. Exp. Biol.* **200**, 225-235.

Montalvetti, A., Rohloff, P. and Docampo, R. (2004). A functional aquaporin co-localizes with the vacuolar proton pyrophosphatase to acidocalcisomes and the contractile vacuole complex of *Trypanosoma cruzi*. *J. Biol. Chem.* **279**, 38673-38682.

Morris, C. E. (2001). Mechano-sensitive ion channels in eukaryotic cells. In *Cell Physiology Sourcebook, A Molecular Approach*, 3rd edn (ed. N. Sperelakis), pp. 745-760. San Diego, San Francisco, New York, Boston, London, Sydney, Tokyo: Academic Press.

Naitoh, Y., Tominaga, T. and Allen, R. D. (1997a). The contractile vacuole fluid discharge rate is determined by the vacuole size immediately before the start of discharge in *Paramecium multimicronucleatum*. *J. Exp. Biol.* **200**, 1737-1744.

Naitoh, Y., Tominaga, T., Ishida, M., Fok, A. K., Aihara, M. S. and Allen, R. D. (1997b). How does the contractile vacuole of *Paramecium multimicronucleatum* expel fluid? Modelling the expulsion mechanism. *J. Exp. Biol.* **200**, 713-721.

Nishihara, E., Shinmen, T. and Sonobe, S. (2004). Functional characterization of contractile vacuole isolated from *Amoeba proteus*. *Cell Struct. Funct.* **29**, 85-90.

Ogden, D. (ed.) (1994). *Microelectrode Techniques, The Plymouth Workshop Handbook*, 2nd edn. Cambridge: Company of Biologists.

Rudy, B. and Iverson, L. E. (ed.) (1992). *Methods in Enzymology*, vol. 207, *Ion Channels*. San Diego, New York, Boston, London, Sydney, Tokyo: Academic Press.

Sheetz, M. P. and Dai, J. (1996). Modulation of membrane dynamics and cell motility by membrane tension. *Trends Cell Biol.* **4**, 85-89.

Sokabe, M., Sachs, F. and Jing, Z. (1991). Quantitative video microscopy of patch clamped membranes stress, strain, capacitance, and stretch channel activation. *Biophys. J.* **59**, 722-728.

Stock, C., Allen, R. D. and Naitoh, Y. (2001). How external osmolarity affects the activity of the contractile vacuole complex, the cytosolic osmolarity and the water permeability of the plasma membrane in *Paramecium multimicronucleatum*. *J. Exp. Biol.* **204**, 291-304.

Stock, C., Grønlien, H. K. and Allen, R. D. (2002a). The ionic composition of the contractile vacuole fluid of *Paramecium* mirrors ion transport across the plasma membrane. *Eur. J. Cell Biol.* **91**, 505-515.

Stock, C., Grønlien, H. K., Allen, R. D. and Naitoh, Y. (2002b). Osmoregulation in *Paramecium*: in situ ion gradients permit water to cascade through the cytosol to the contractile vacuole. *J. Cell Sci.* **115**, 2339-2348.

Tani, T., Allen, R. D. and Naitoh, Y. (2000). Periodic tension development in the membrane of the *in vitro* contracile vacuole of *Paramecium multimicronucleatum*: modification by bisection, fusion and suction. *J. Exp. Biol.* **203**, 239-251.

Tani, T., Allen, R. D. and Naitoh, Y. (2001). Cellular membrane that undergo cyclic changes in tension: Direct measurement of force generated by an *in vitro* contractile vacuole of *Parmecium multimicronucleatum*. *J. Cell Sci.* **114**, 785-795.

Tani, T., Tominaga, T., Allen, R. D. and Naitoh, Y. (2002). Development of periodic tension in the contractile vacuole complex membrane of *Paramecium* governs its membrane dynamics. *Cell Biol. Int.* **26**, 853-860.

Tominaga, T., Allen, R. D. and Naitoh, Y. (1998a). Electrophysiology of the *in situ* contractile vacuole complex of *Paramecium* reveals its membrane dynamics and electrogenic site during osmoregulatory activity. *J. Exp. Biol.* **201**, 451-460.

Tominaga, T., Allen, R. D. and Naitoh, Y. (1998b). Cyclic changes in the tension of the contractile vacuole complex membrane control its exocytotic cycle. *J. Exp. Biol.* **201**, 2647-2658.

Tominaga, T., Naitoh, Y. and Allen, R. D. (1999). A key function of non-planar membranes and their associated microtubular ribbons in contractile vacuole membrane dynamics is revealed by electrophysiologically controlled fixation of *Paramecium*. *J. Cell Sci.* **112**, 3733-3745.

Wieczorek, H., Brown, D., Grinstein, S., Ehrenfeld, J. and Harvey, W. R. (1999). Animal plasma membrane energization by proton-motive V-ATPases. *BioEssays* **21**, 637-648.

Yoshida, K., Ide, T., Inouye, K., Mizuno, K., Taguchi, T. and Kasai, M. (1997). A voltage- and K^+-dependent K^+ channel from a membrane fraction enriched in contractile vacuole of *Dictyostelium discoideum*. *Biochim. Biophys. Acta* **1325**, 178-188.